Davidson, J. & Boghrat, A. 1983. Displacements and Strains around Probes in Sand. Proc. ASCE Spec. Conf. on "Geotechnical Practice in Offshore Engineering". Austin, Texas, p. 181-203. Apr.

From Paris conf. May 83

PLEASE RETURN TO JOHN H. SCHMERTMANN

Rec'd 5 Apr 83

DISPLACEMENTS AND STRAINS AROUND PROBES IN SAND

By John L. Davidson,[1] M ASCE and Alireza Boghrat[2]

INTRODUCTION

In the past decade the use of insitu testing for geotechnical purposes, both onshore and offshore, has increased dramatically. Compared to the traditional drilling, sampling and laboratory testing procedures, insitu testing has several important benefits. These are that insitu tests are performed in the natural environment of moisture and stress, with reduced disturbance and on large volumes of soil. They are also generally quicker and cheaper, relative to the quantity of data acquired. New pieces of insitu test equipment with increasing sophistication and capabilities are continually coming onto the market.

This paper seeks to compare and evaluate two standard shapes of insitu test equipment. The first shape, the 'cone', is a 35.7 mm diameter cylindrical rod with a 60° apex cone, Figure 1. This is the shape of the standard electric Cone Penetration Test tip (14) and of many of the available piezocones (e.g. 7, 10, 16, 17), Figure 2. The second shape, the 'blade', is a flat plate 235 mm x 95 mm x 14 mm, with a bevelled lower end and a threaded connector, Figure 1. This is the shape of the Marchetti dilatometer (12, 13) and of the University of Florida piezoblade (3), Figure 3.

Both cone penetration tests and piezocone tests are standard offshore investigation tools, performed from a ship or barge, from a sea floor system (9) or from a deep submersible (11). Dilatometer tests have also been performed from barges. Dr. Marchetti has tested in water depths up to 30 meters to total depths of 60 meters. The device was also used recently by Schmertmann and Crapps, Inc. during site investigation for the Sunshine Skyway bridge in Tampa, Florida.

Since these types of tests are performed by penetrating a solid probe into the ground, a certain disturbance of the soil results. The magnitude, location and type of disturbance are all important in evaluating the usefulness and reliability of the test.

This paper describes a laboratory testing technique which allows a determination of the displacements and strains around a penetrated

---

1. Associate Professor, Department of Civil Engineering, University of Florida, Gainesville, Florida.

2. Graduate Assistant, Department of Civil Engineering, University of Florida, Gainesville, Florida.

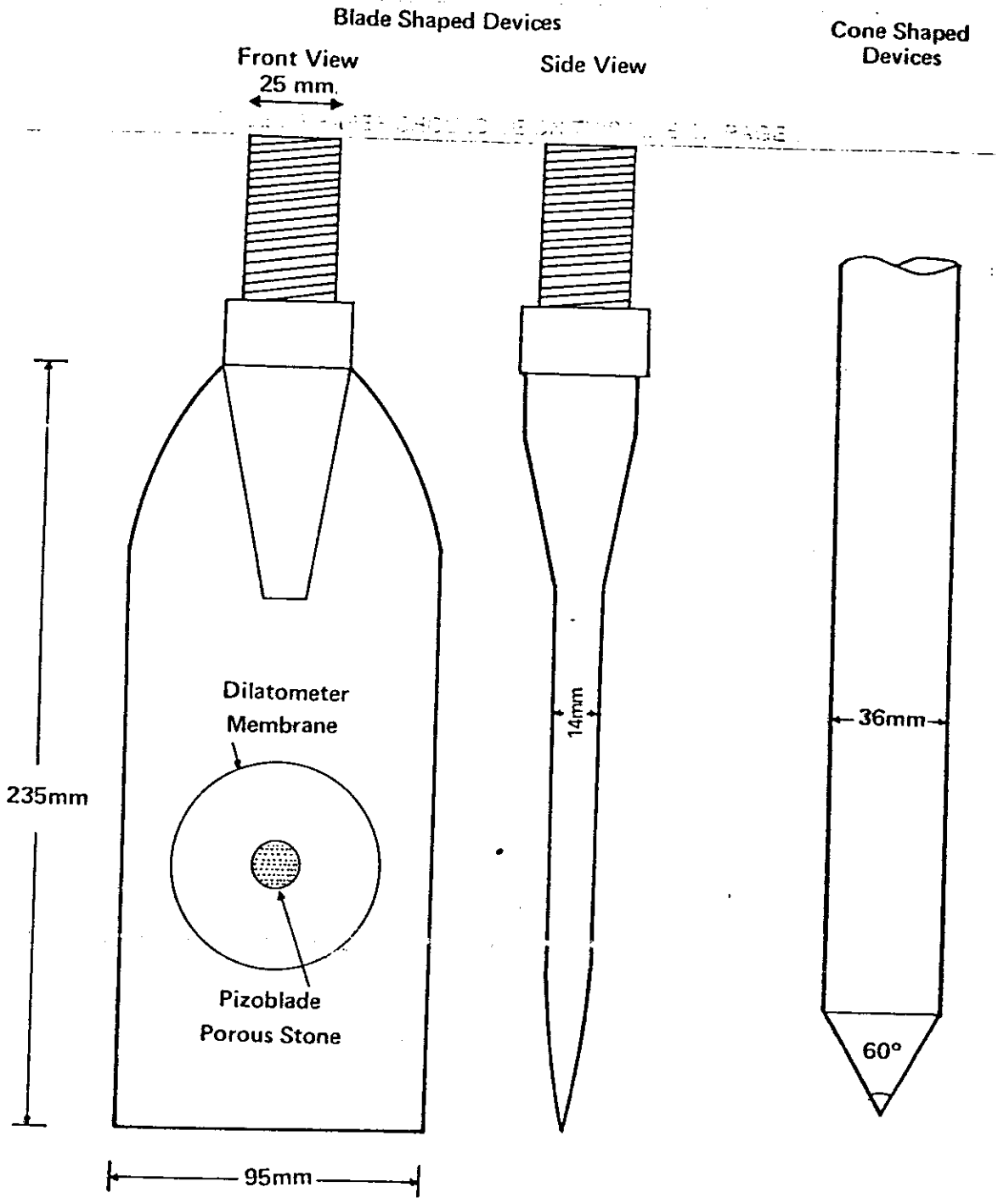

Figure 1. Sketches of the Blade and Cone

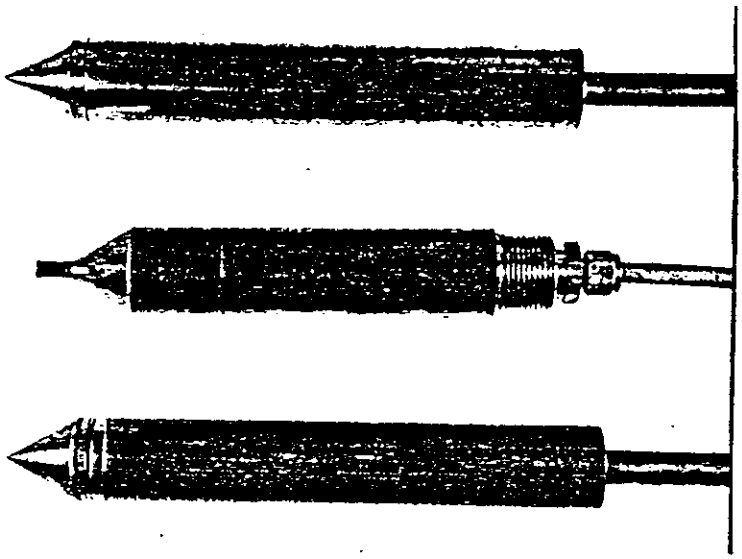

Figure 2. Electric Cone Tip, Wissa Piezocone and Fugro Piezocone

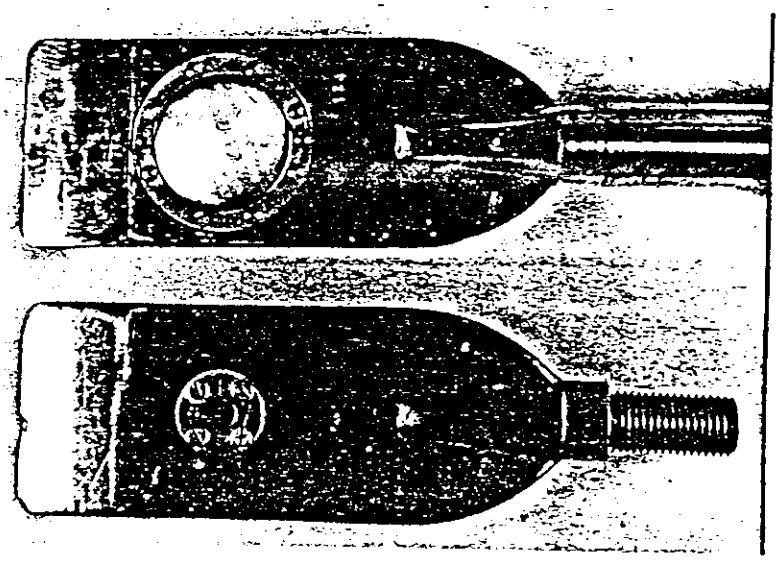

Figure 3. Marchetti Dilatometer and University of Florida Piezoblades

probe. The two standard shaped probes were tested in this manner, and are compared with regard to the disturbance caused around each during insertion.

The tests reported in this paper are all of shallow penetration - for the cone, the penetration tip depth to diameter ratios are only 6 and 8 - for the blade, the depth to width ratios are 16. A few tests have been performed in which the sand surface has been surcharged to simulate depth, but are not reported herein.

This paper is an extension of an earlier paper (6) in which the testing technique was briefly described and in which penetration of the cone shaped probe into two different density sands was reported.

PSEUDO STEREO TECHNIQUE

In conventional aerial stereo photography methods, two photographs of an object are taken from slightly different camera positions. These photographic plates are then positioned in a stereo projector and a stereoscopic image obtained. Figure 4 illustrates the taking of such photographs and the corresponding stereo image obtained by a simultaneous projection of the plates. The height of the object in the stereo image is due to the difference in locations of the corresponding points in the two photographs, called x-parallax. This is the basic principle of stereo photography.

Parallax can also be produced by keeping the camera position stationary and photographing the displacement of an object. Figure 5 illustrates a fixed camera photographing a translated object and the stereo image obtained by a simultaneous projection of these plates. The height of the stereo image depends on the magnitude of the x-movement.

If the object undergoes a general planar displacement, i.e., movement components in two directions, only the component of displacement along the line joining the projectors contributes to the elevated stereo image. In order to completely define an actual displacement, two measurements must be made. The component of the displacement is first measured in any particular direction by positioning the photographic plates in the projector so that the line connecting the two plates is parallel to that direction. The plates are then rotated 90° in order to determine the perpendicular component of movement. The actual magnitude and direction of the displacement is then obtained by a vector sum of these normal components. This technique, called pseudo stereo photgraphy, was pioneered at the University of Southampton, U. K. (1, 4).

TEST EQUIPMENT AND PROCEDURE

A wooden container with one glass wall was constructed, with inside dimensions of length 100 cm, width 50 cm and height 65 cm. The inside volume, measuring to the level to which the sand was usually placed, was 0.267 m^3 (9.44 ft^3). A square grid or static datum plane was scored on the inside face of the glass. The middle third of the glass length had

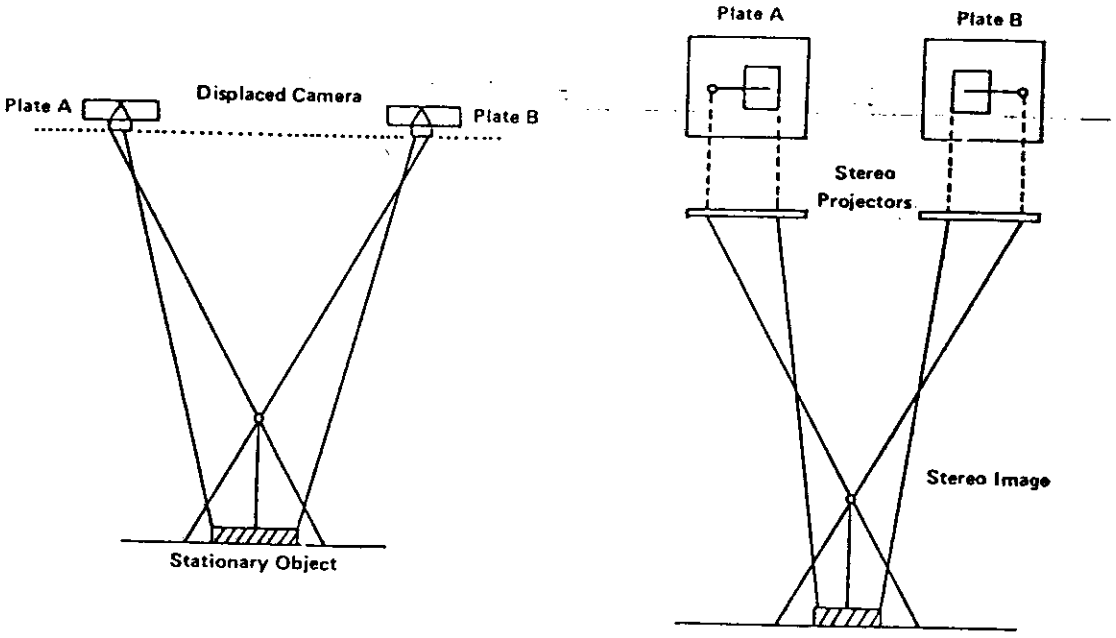

Figure 4. Stereo Image - Displaced Camera

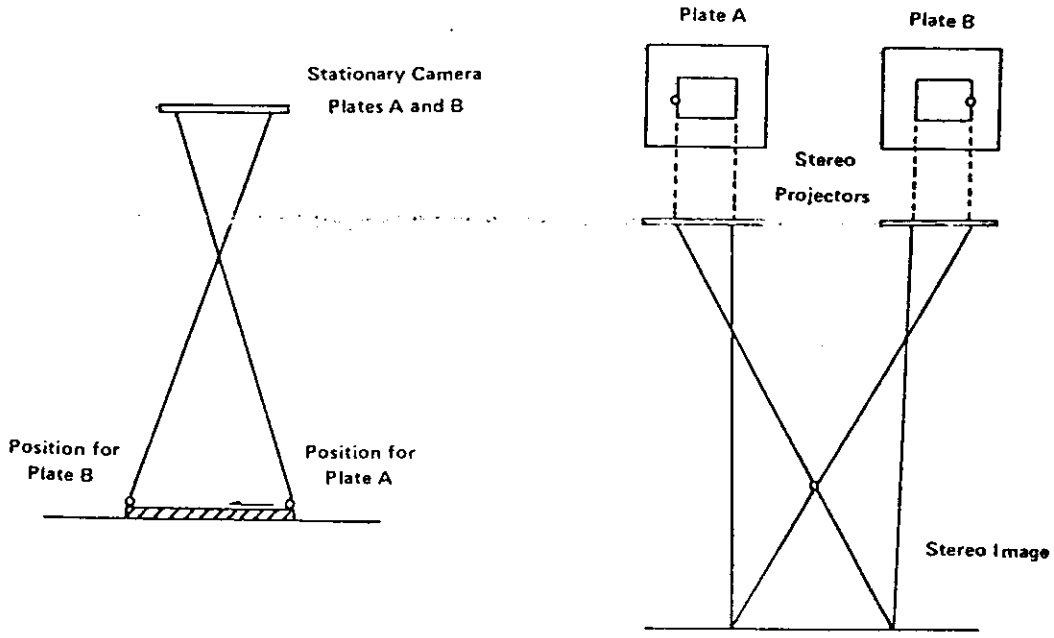

Figure 5. Stereo Image - Displaced Object

a 15 mm x 15 mm square grid, while the two outer thirds had 30 mm x 30 mm grids. Before each test, the grid was darkened with a black marker, so that it could be more easily seen on the photographs and in the stereo image.

The sand used in the research was a blend of four graded sands; 8/20, 20/30, 30/64 and EGS, from the Edgar Plastic Kaolin Company, Florida. The pairs of numbers, e.g. 20/30, signify the sieve size range in which 75% or more of the soil particles lie. The blend had an effective size D_{10} of 0.2 mm and a unformity coefficient C_u of 7. The sand was placed in the container and tests performed at five different densities, obtained by different filling and mechanical compaction procedures.

Dummy cone and blade probes were machined from stainless steel, then cut longitudinally in half, Figure 6. The test procedure consisted of penetrating a probe into the sand with the flat, cut face against the glass, Figure 7. A small hydraulic jack was employed. A series of 6 or 8 photographs were taken - one prior to penetration, and the rest during penetration - from a rigidly fixed camera. Figure 8 shows the test set-up.

The three-dimensional problems are thus studied by physically cutting the probes and viewing a two-dimensional plane - a radial plane in the case of the axisymmetrical cone and a plane strain plane in the case of the blade. Direct shear tests were performed to measure the friction between the sand and the glass of the container wall. For a dense sand (ϕ=40^0) a friction angle of 14° was found for smooth glass and 16.5° for a plate scored with the 15 mm grid (5).

To avoid possible distortion of parallax due to quality of photographic paper or the enlargement process, photographic positives were used rather than prepared prints. The positive slides were sandwiched between thin, clear photographic glass plates and used directly in the stereo plotter. The camera was fixed in position relative to the model, with its optical axis normal to the displacement plane. A B & J orbit view camera with a 4" x 5" plate holder was used with Ektachrome 50 Professional Tungsten Film. After each test the container was carefully emptied, the sand weighed and the bulk density determined.

For analysis of each pair of test photographs, a Fotocartigrafo Nistri Model VI double-projection anaglyphic plotter was used, Figure 9. This type of plotter employs the anaglyph principle of projection of light of two complementary colors, red and blue-green, to create the stereo image. The overlapping image created by projecting through two photographic plates is viewed through glasses with one red and one blue-green lens. Since each eye sees only one of the photographs of the pair, the three-dimensional effect is created. The portion of the photographs which is of interest is projected onto the white surface of a moveable platen assembly. A small white dot on the platen which, when viewed through the glasses, appears to be floating in space, can be moved vertically and placed on the surface of the 3-D model.

Figure 6. The Test Probe and Blade

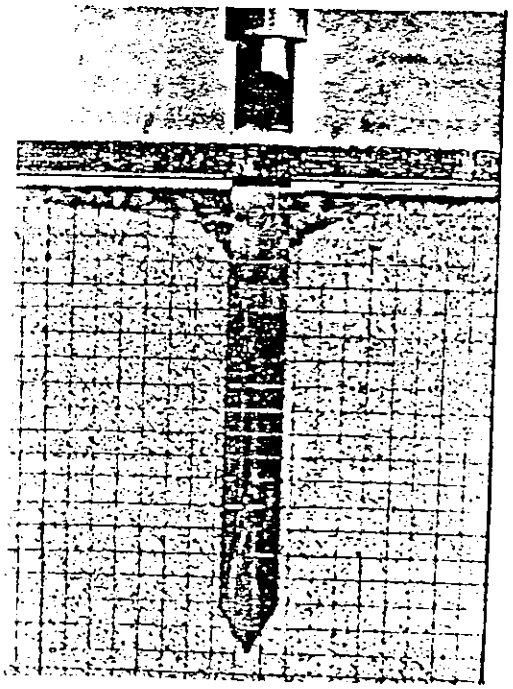

Figure 7. Probe Penetrated into Sand

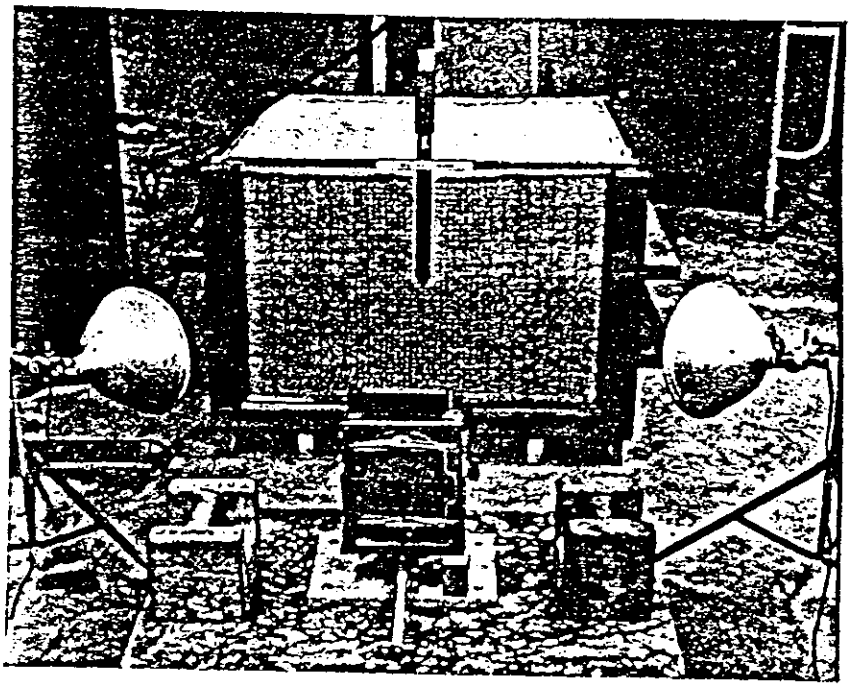

Figure 8. Test Set Up

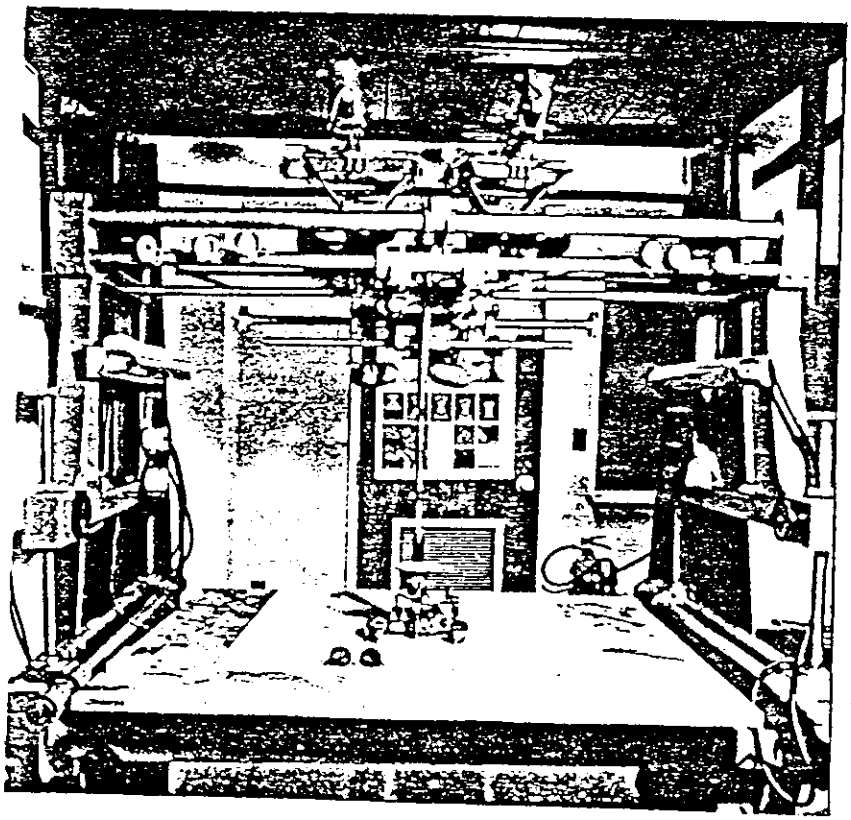

Figure 9. Double Projection Anaglyphic Plotter

Figure 10 shows two pairs of stereo photographs. Two readings are taken at each grid point. The floating dot is first placed on the grid and a reading from the platen dial recorded. The dot is then placed on the sand, which may appear above or below the stationary datum grid, and a second reading taken. The difference in these readings is a measure of how far the sand moved at that point, during the time between photographs, in the direction parallel to the line of the projectors.

The grid scored on the glass was numbered in finite element terminology with 1234 node points and 1213 elements. At each node point where sand movement had occurred, the two floating dot readings were recorded and subsequently entered as data for a computer reduction program. Each pair of photographs was viewed twice to provide orthogonal displacements which could be summed to give the actual movement vector.

Displacements were determined by

$$U \text{ or } W = C \cdot \Delta h$$

where

U = horizontal displacement in millimeters
W = vertical displacement in millimeters
Δh = difference in floating dot grid and sand readings
C = constant which is a function of the stereo plotter set-up
= 0.012958 for the cone study
= 0.016402 for the blade study

$$D = \sqrt{(U^2 + W^2)}$$

$$\theta = \tan^{-1} (W/U)$$

where

D = actual displacement
θ = angle of displacement from horizontal

Volumetric strains were defined for each element by

$$\varepsilon_v = \frac{\Delta V}{V}$$

where

ε_v = volumetric strain
ΔV = change in volume
V = original volume

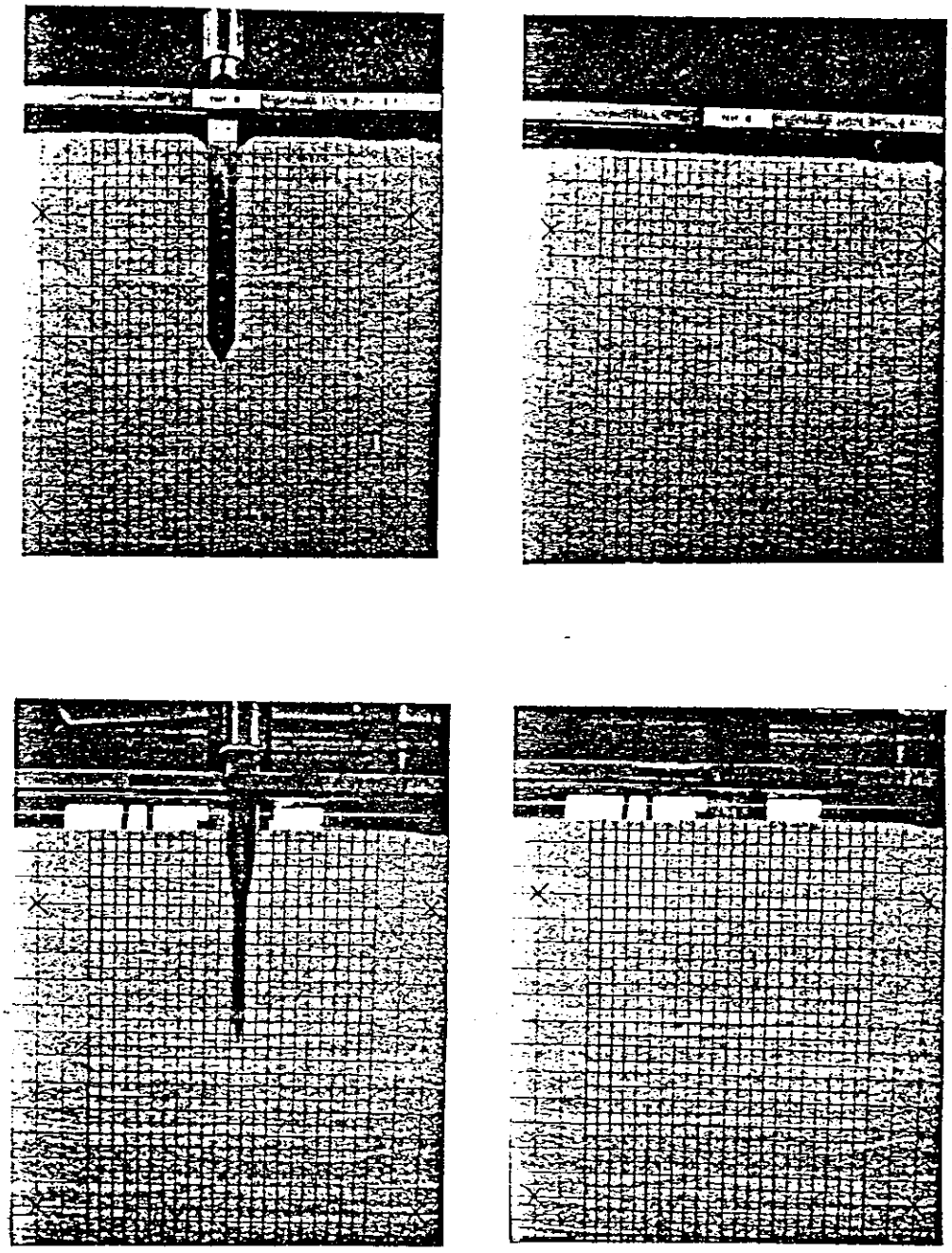

Figure 10. Two Stereo Pairs

In the case of the blade shaped device, plane strain conditions were assumed to apply, since the width to thickness ratio was 6.8. The volumetric strain was therefore defined as

$$\varepsilon_v = \frac{A - A_o}{A_o}$$

where

A_o = original area of a grid element
A = deformed area of an element defined by the ends of the four corner node point displacements, D.

For the case of the axisymmetrical cone the effect of the tangential strains must be included. The volumetric strain was therefore calculated using the equation

$$\varepsilon_v = \frac{V - V_o}{V_o}$$

where

V_o = the volume found by revolving the original underformed square grid element around the axis of symmetry
V = the volume found by revolving the deformed quadrilateral element around the same axis

A decrease in area or volume, i.e., compression, was defined as a positive volumetric strain, while an increase was defined as negative.

Shear strains were determined at each node point by

$$\gamma_{xz} = (\gamma_{xz_2} + \gamma_{xz_4})/2$$

where

γ_{xz_2} = shear strain in the 2nd quadrant grid element, node at the origin
γ_{xz_4} = shear strain in the 4th quadrant grid element, node at the origin

$$\gamma_{xz_i} = \alpha_i + \beta_i$$

where

i = 2 or 4

α = the change in direction of the horizontal side of the element at the node point, in radians

β = the change in direction of the vertical side of the element at the node point, in radians

An increase in the original right angle was defined as a negative shear strain and a decrease in angle was defined as positve.

The accuracy of the stereo measurements were checked by multiple reading of the parallaxes at several node points, especially close to the probe where grain movement is large. The variation found translates into a maximum error of ±7% in the displacement vectors (5) and corresponding errors of similar magnitude in the volumetric and shear strains. Andrawes and Butterfield (1) were able to measure individual grain displacements to an accuracy of better than 0.005 mm.

A detailed description of the test equipment and procedures, and of the computer reduction program, can be found in a report by Davidson (5).

RESULTS

In this research program, ten laboratory penetration tests were performed, using two different probes and five different density soils. In this paper, because of length restrictions, only four of these tests, the two probes in two different soils are reported. The 'loose' sand was placed, using a 3/4" funnel held 5-7 inches above the sand surface. The 'dense' sand was placed in 4 inch lifts, using the same method. Each lift was then compacted with 5 passes of a mechanical compactor.

Only one pair of photographs from each of these four tests is analyzed. One photograph is of the sand prior to insertion, the other is the last photograph taken, at final penetration, Figure 10.

Three figures are plotted for each of the four tests. These are node point displacement vectors, contours of volumetric strain and contours of shear strain. Since the probes are both symmetrical, results are plotted for only half the problem, the right hand side.

Individual tests will first be discussed and then the cone and blade will be compared.

Cone - Loose Sand (Figure 11)

All the displacements are to the right and down, away from the cone. The vectors are all directed at angles less than 45° to the horizontal, except in a bulb shaped zone beneath the tip. The largest displacement measured was approximately 4 mm. The effect of the cone was measurable outward to a distance of 125 mm from the edge of the probe and downward 135 mm below the tip.

Negative volumetric strains were detected below the tip and immediately adjacent to the shaft of the cone. Minor irregular densification was observed further from the probe.

The shear strains are primarily negative (increase in right angle) except for a number of very low positive readings directly below the cone tip. The strains are fairly uniform adjacent to the probe shaft and except for one small pocket are small, less than -2%. Adjacent to the tip is a bulb of high negative shear straining with a maximum reading of 10%.

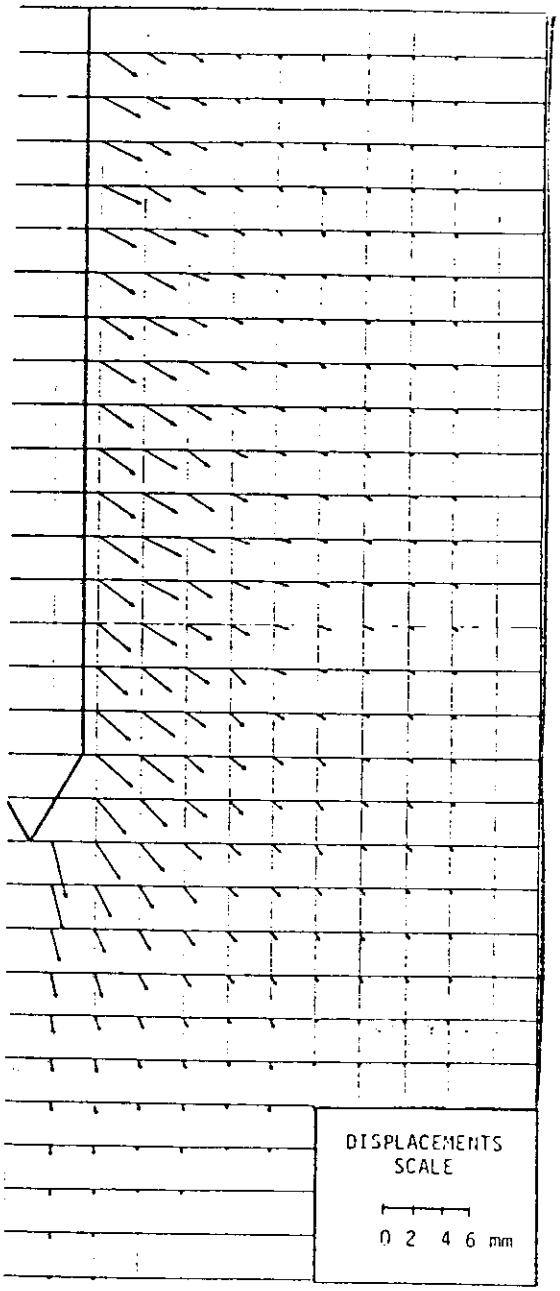

Figure 11a. Cone - Loose
Displacements

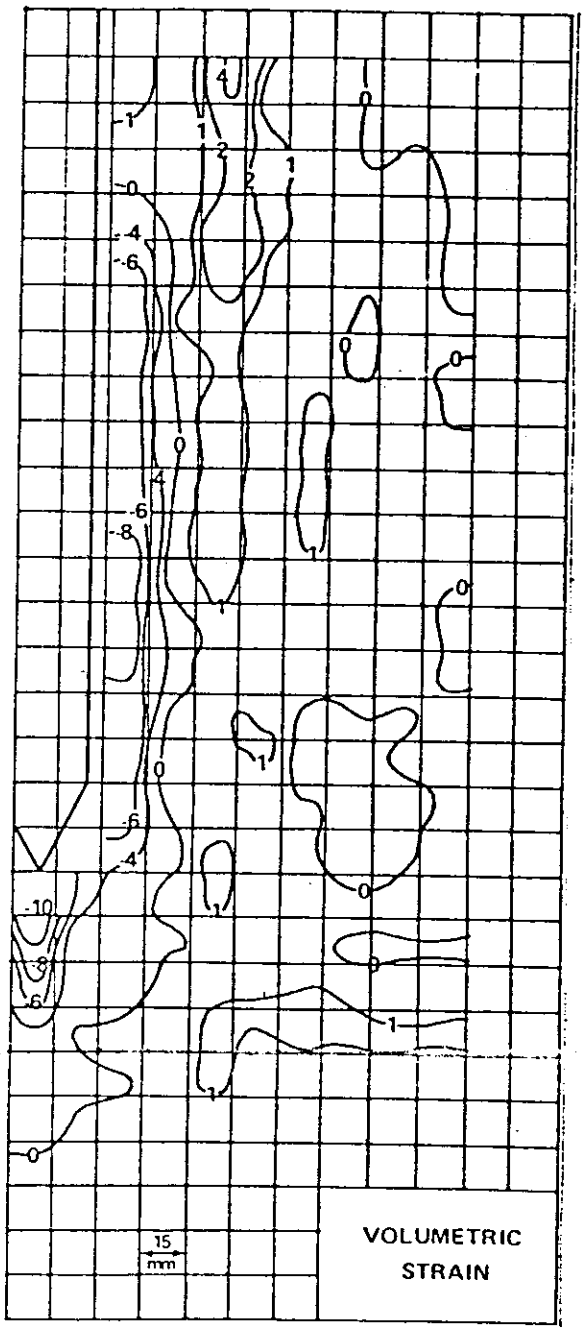

Figure 11b. Cone - Loose
Volumetric strains

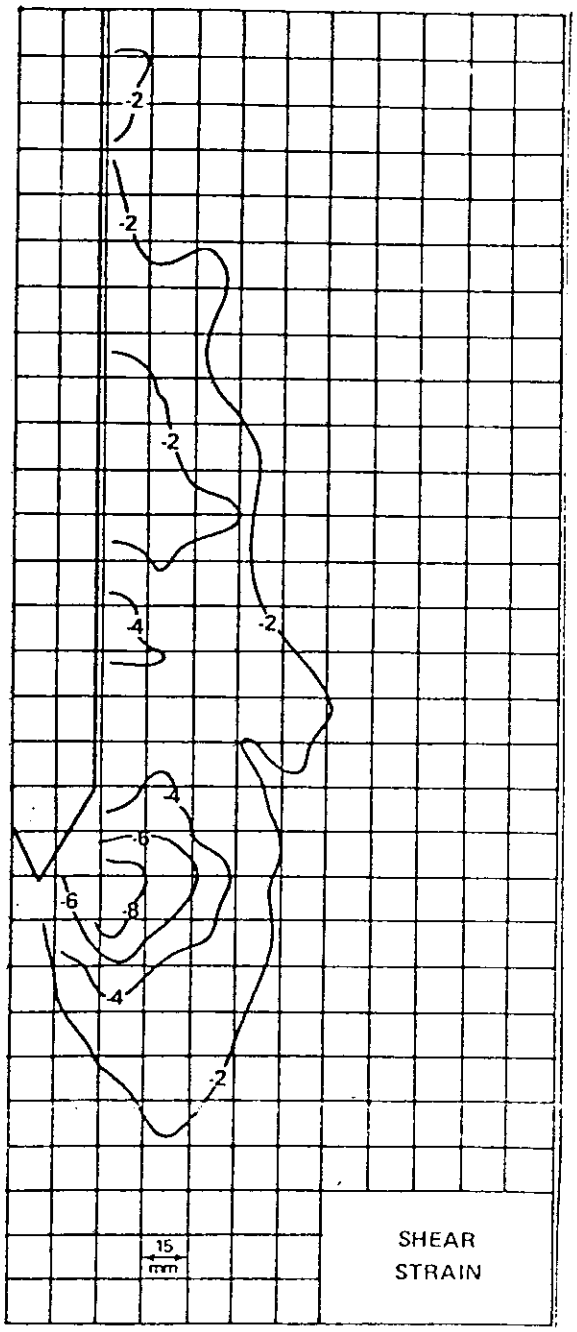

Figure 11c. Cone - Loose
Shear strains

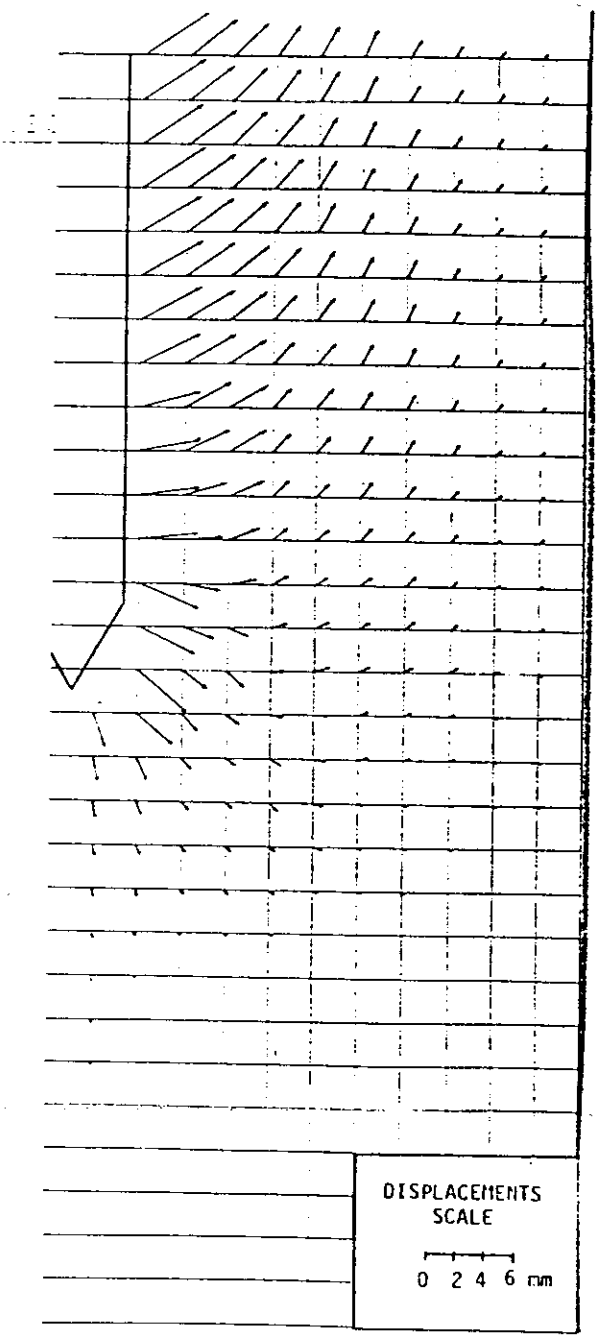

Figure 12a. Cone - Dense
Displacements

Cone - Dense Sand (Figure 12)

The displacement vectors for the dense sand show a downward and outward movement below the cone tip, and an upward and outward movement above the tip. There is a noticeable pattern of curved surfaces of particle movement from the probe to the sand surface. The maximum displacement is approximately 5 mm. Displacements were measurable horizontally to 155 mm, and vertically to 100 mm below the tip.

For this sand, negative volumetric strains are detected below the tip and along the shaft. However, unlike the loose sand, a zone of densification (ε_v = +6%) is found adjacent to the tip.

As in the loose sand, the shear strains are primarily negative. Again, a concentration of straining is found adjacent to the tip, in this case of maximum magnitude -12%. Along the shaft the strains are slightly higher ($\approx$ -4%), becoming positive as the soil surface is approached.

Blade - Loose Sand (Figure 13)

Displacements in this loose sand are all to the right and down, away from the probe. Movements were measurable to 100 mm from the edge of the probe and downward below the tip. The maximum particle displacement adjacent to the flat surface of the probe is 2.2 mm.

The volumetric strain readings are all positive except for a few negative values directly below the tip. The contours are very uniform adjacent to the blade face, showing decreasing densification with distance from the probe.

The shear strains are all negative, except for some low positive values on the symmetry line below the tip. Adjacent to the blade's flat surface the shear strains are very uniform, decreasing from $\approx$ -2.5% to zero with distance from the probe.

Blade - Dense Sand (Figure 14)

The displacement vectors for this test show outward and upward movements, except below the probe tip level, where downward movement occurs. A very sharp distinction exists at the tip level. The outward movement was measurable to a distance of 160 mm from the edge of the probe and down to a depth of 90 mm below the tip. The maximum movement adjacent to the flat area of the probe is 3.6 mm.

The volumetric strain readings are all positive, except for two small zones directly below and adjacent to the tip. The contours are again very uniform in the soil adjacent to the flat surface of the blade, decreasing from 4% with distance from the probe. The contour pattern is more complex around the tip and near the width enlargement, or shoulder, at the top of the blade.

The shear strain contours show zones of both positive and negative straining. Positive shear strains are observed below the tip, and adjacent to the blade's flat surface, decreasing here from $\approx$ 1% to zero

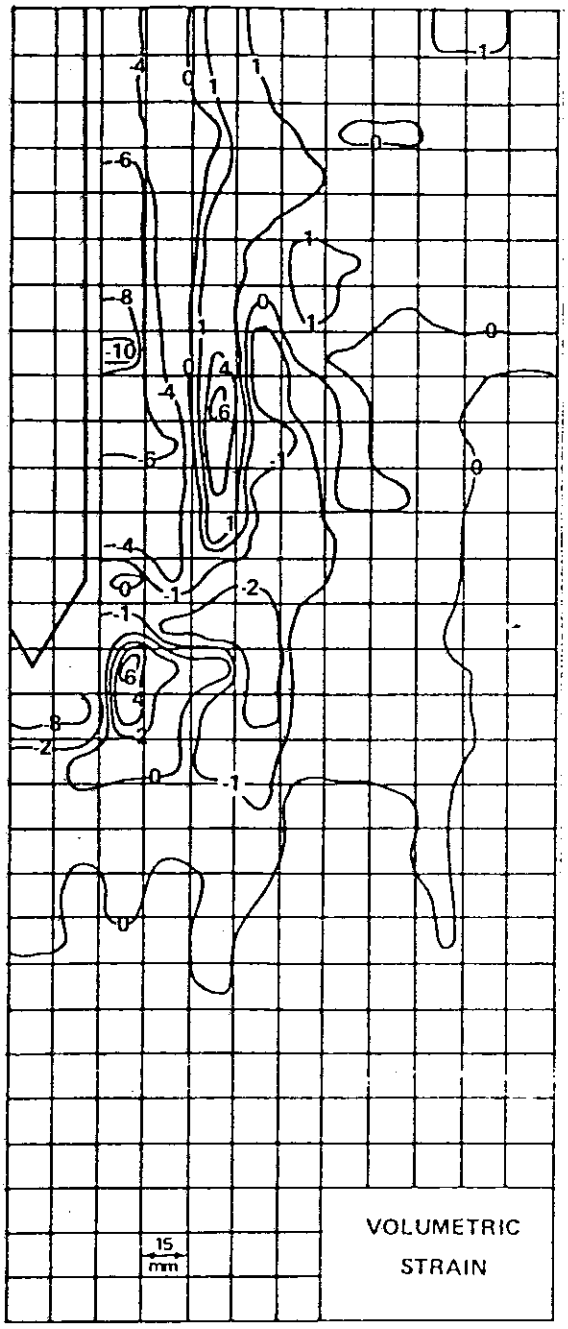

Figure 12b. Cone - Dense
Volumetric strains

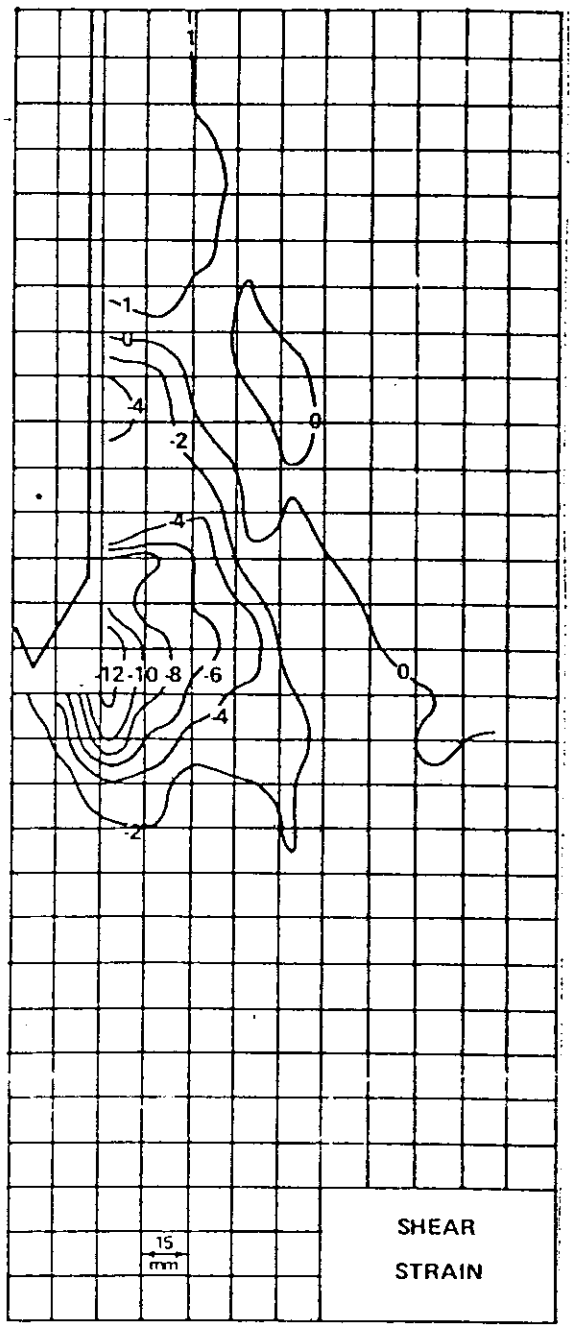

Figure 12c. Cone - Dense
Shear strains

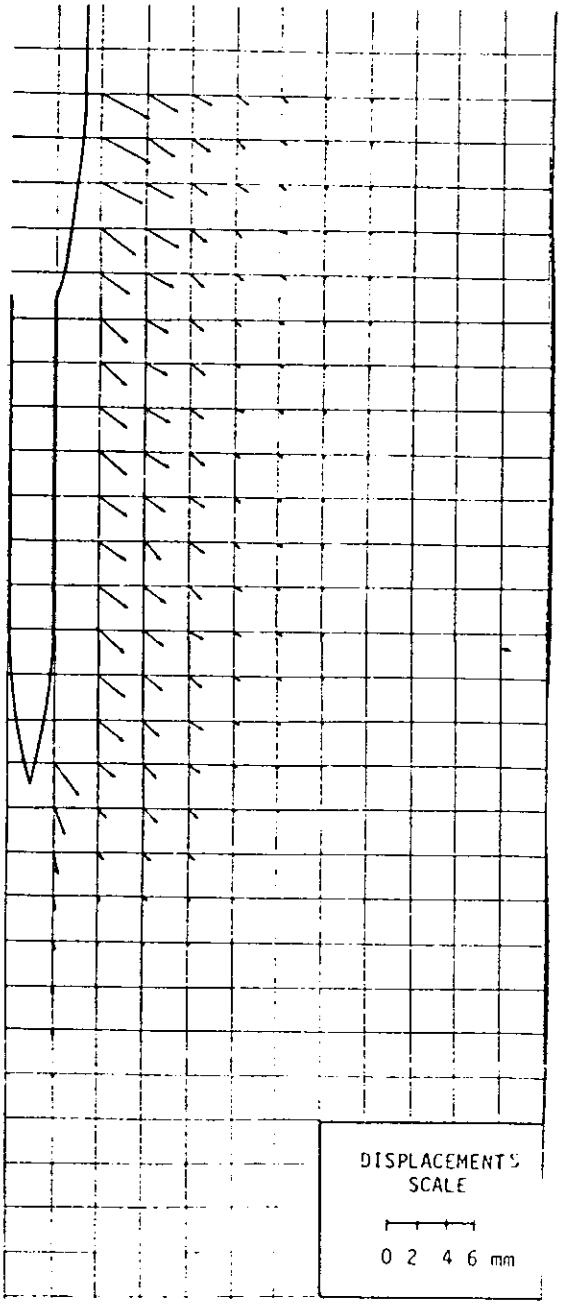

Figure 13a. Blade - Loose
Displacements

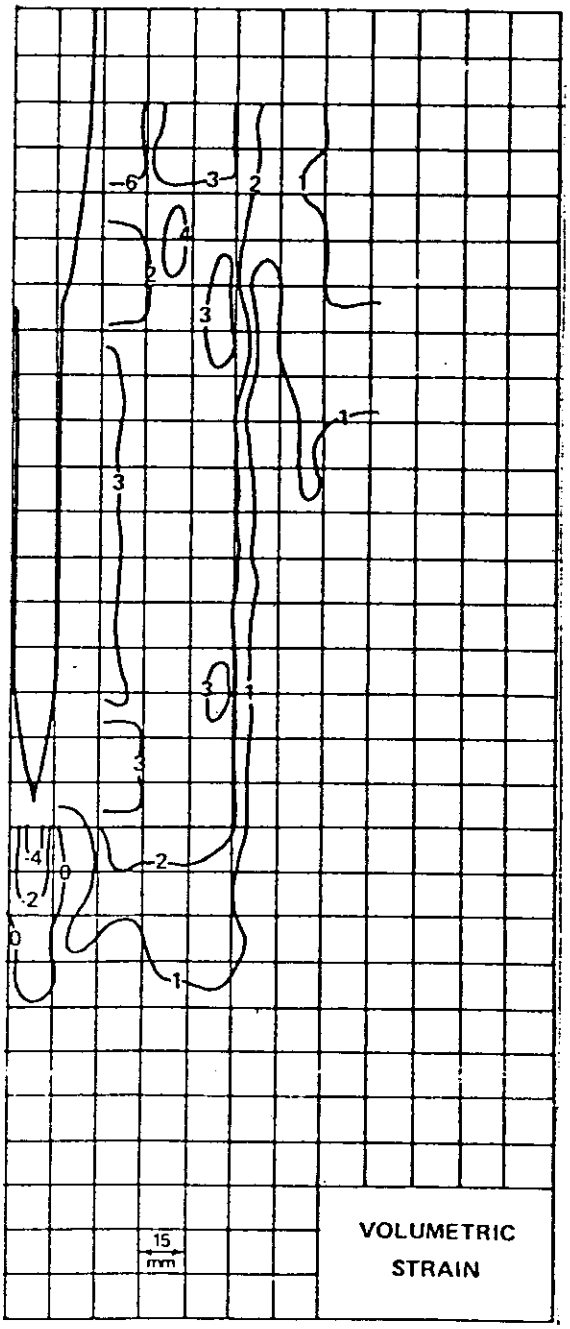

Figure 13b. Blade - Loose
Volumetric strains

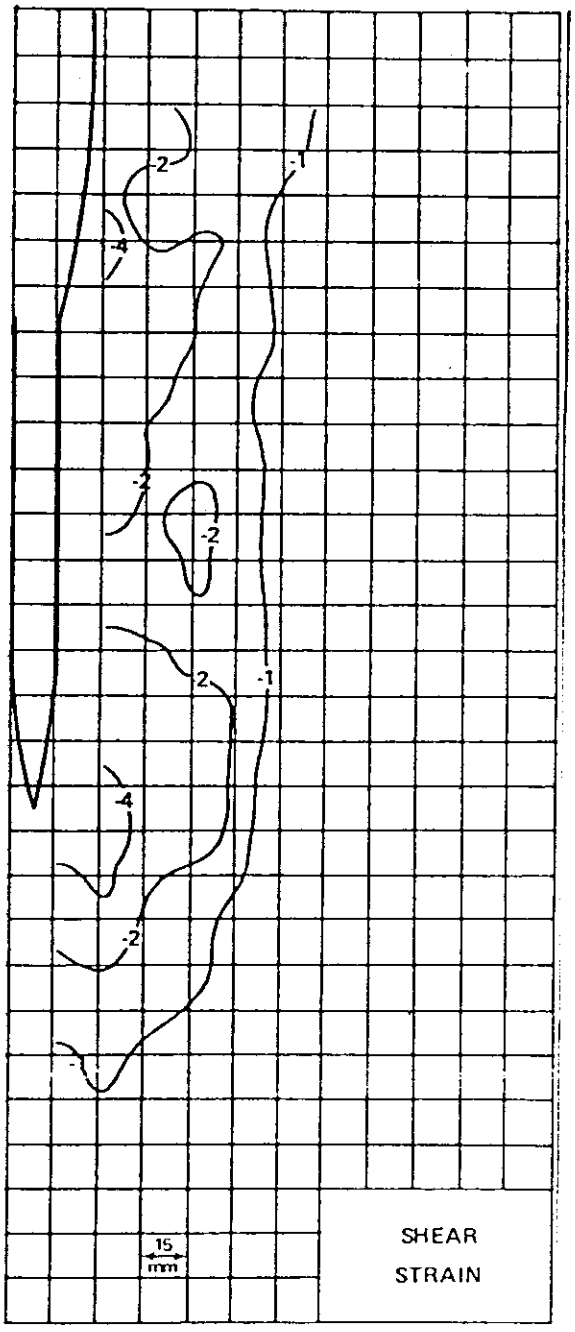

Figure 13c. Blade - Loose
Shear strains

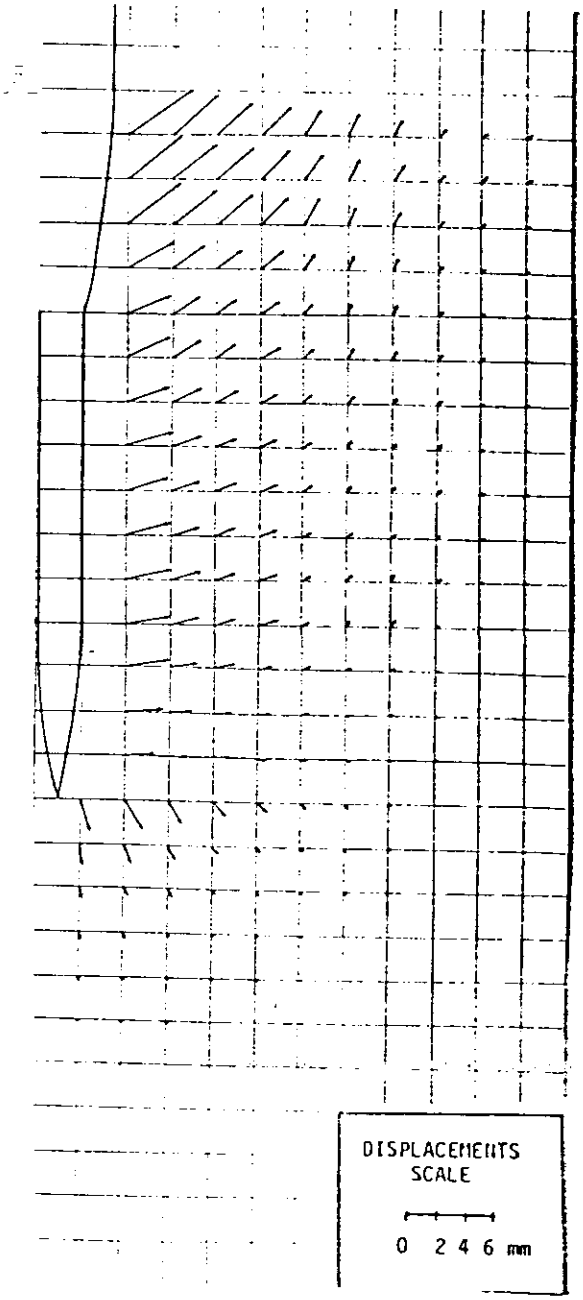

Figure 14a. Blade - Dense
Displacements

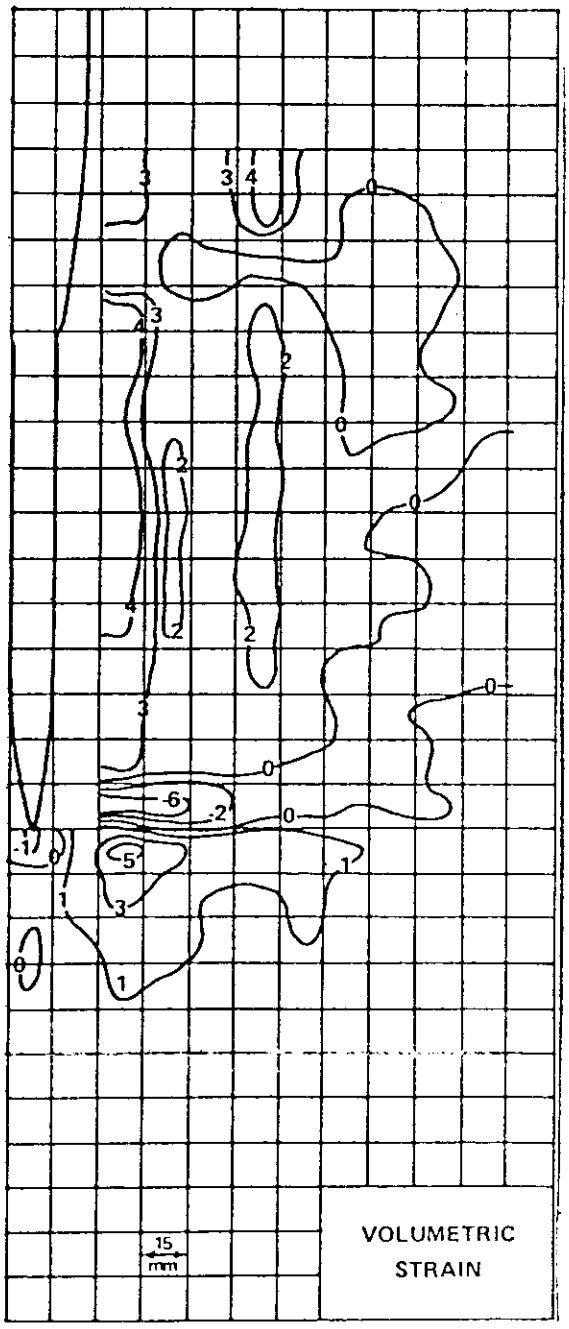

Figure 14b. Blade - Dense
Volumetric strains

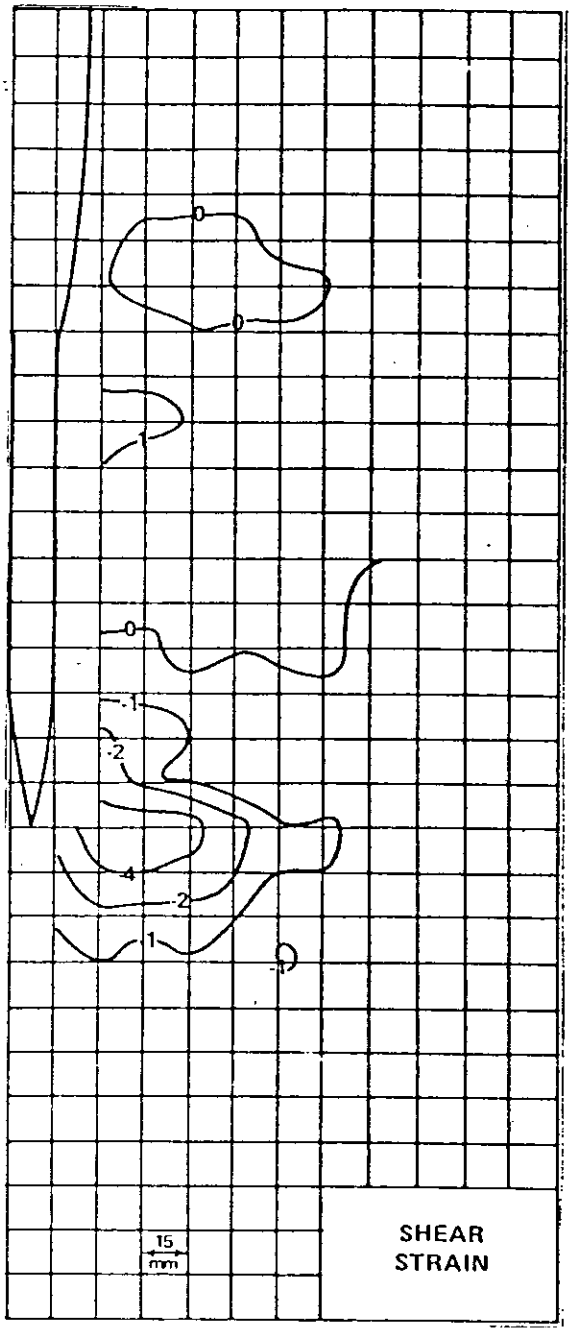

Figure 14c. Blade - Dense
Shear strains

with distance. A zone of negative shear strain, maximum value -5%, is found adjacent to the bevelled region at the bottom of the blade. A small negative zone is located near the blade shoulder.

COMPARISON OF CONE AND BLADE

Displacement

In the loose sand, both probes produced downward and outward displacement only. Near the top of the probes the movements were of the same order of magnitude. This was to be expected, since the enlarged blade width is 35 mm, while the cone diameter is 35.7 mm. Adjacent to the flat, 14 mm thick, blade surface and around the tip, the displacements were considerably smaller than for the cone shaped instrument.

Similar results were obtained in the dense sand. In general, displacements were smaller for the blade shaped device. In the dense sand, the y-direction of the movement, up or down, changes for both probes. For the blade, only the soil below the actual tip level moved downward, while in the cone the change of direction occurred just above the top of the conical tip.

Volumetric Strains

In loose sands, the cone produced an unexpected zone of loosening around the tip and shaft. Such results are somewhat corroborated by Schmertmann (14), who measured negative pore pressures with a piezocone during field testing in loose sand.

In dense sands, the cone generated high negative volumetric strains adjacent to the tip and shaft, and a zone of positive strain adjacent to the tip.

In both loose and dense sands, the blade showed very uniform volumetric strains adjacent to the flat surface and some concentrations of strain near the tip and the shoulder.

Shear Strains

For both probes, in the loose sand, shear strains were negative everywhere except directly under the tips. Adjacent to both the cone and the blade tips were high concentrations of negative shear strain. Along the cone shaft and the blade face, the shear strains were uniform and of approximately the same magnitude.

In the dense sand, both probes generated positive shear strains under the tip and along the upper shaft and blade surfaces. The cone had a very negative concentration adjacent to the tip, which extended part way up the shaft. The blade had much lower negative shear strains adjacent to the bevelled section and low uniform positive strains adjacent to the flat surface.

Conclusions

The laboratory tests were performed on solid steel dummy probes. However, to evaluate particular pieces of insitu test equipment, consideration must be given to the actual location of the measuring devices. In the blade instruments, the expanding circular membrane of the Marchetti dilatometer and the porous disc of the University of Florida piezoblade are located on the flat, 14 mm thick surface, Figure 1. In the piezocone, the porous sensing element is either a small cylindrical element at the point of the tip, (8, 10, 18) or is located on the surface of the tip or on the shaft above the tip (7, 16, 17)

For the dilatometer and piezoblade, in the region where measurements are made, displacements are small and uniform (maximum recorded values: 2.2 mm in loose, 3.6 mm in dense), volumetric strains are very uniform (maximum recorded values: 3% in loose, 4% in dense) and shear strains are very uniform (maximum recorded values: -2.5% in loose, 1.3% in dense).

Around the tip, where piezocone measurements are made, there appear to be very severe concentrations of straining. In the dense sand, volumetric strain varied around the tip from -9% to +6% and shear strains from slightly positive to less than -12%. In loose sand the shear strains varied from 0% to -10%. The volumetric strains did not vary excessively in this test, between -6% and -10%.

Since these strain contours represent a measure of soil disturbance, the blade shaped instrument, with measuring devices on the flat surface, appears to test a much less disturbed soil than do the cone shaped instruments.

The pseudo stereo photograph technique can be used to very accurately measure the displacements of sand grains at designated points in a viewed plane. In this paper both volumetric and shear strains were then calculated based on simple small strain theory, and displacement vectors and strain contours carefully drawn. Conclusions have been drawn based on the numerical values determined and on the trends visible in the plots. However, since extensive duplication of testing has not been performed, the authors do believe that the reported results should be more qualitatively than quantitatively regarded. Possible non-homogeneity and non-reproductibility of the large samples, vibrations, non-vertical penetration, random stereo reading errors etc. can not be entirely discounted.

REFERENCES

1. Andrawes, K. Z. and Butterfield, R., "The Measurement of Planar Displacements of Sand Grains," Geotechnique, Vol. 23, 1973, pp. 571-576.
2. Battaglio, M., Jamiolkowski, M., Lancellotta, R., and Maniscalco, R., "Piezometer Probe Test in Cohesive Deposits," Proceeding, ASCE National Convention, St. Louis, MO, 1981, pp. 284-301.

3. Boghrat, A., "The Design and Construction of a Piezoblade and an Evaluation of the Marchetti Dilatometer in Some Florida Soils," Ph.D. Dissertation, University of Florida, December, 1982.
4. Butterfield, R., Harkness, R. M., and Andrawes, K. Z., "A Stereo Photogrammetric Technique for Measuring Displacement Fields," Geotechnique, Vol. 20, 1970, pp. 308-314.
5. Davidson, J. L., "A study of Deformations in Sand Around a Penetrated Probe Using Stereo Photography," Report, National Science Foundation, ENG76-18849, 1980, 111 pages.
6. Davidson, J. L., Mortensen, R. A. and Barreiro, D., "Deformation in Sand Around a Cone Penetrometer Tip," Xth ICSMFE, Stockholm, Vol. 2, June, 1981, pp. 467-470.
7. deRuiter, J., "Electric Penetrometer for Site Investigation," Journal of the Soil Mechanics and Foundations Division, ASCE, Vol. 97, No. SM2, February, 1971, pp. 457-472.
8. Franklin, A. G. and Cooper, S. S., "Tests in Alluvial Sand with the PQS Probe," Xth ICSMFE, Stockholm, Vol. 2, June, 1981, pp. 475-478.
9. Ferguson, G. H., McClelland, B., and Bell, W. D., "Seafloor Cone Penetrometer for Deep Penetration Measurements of Ocean Sediment Strength," Paper No. OTC 2787, 9th Offshore Technology Conference, Houston, TX, 1977.
10. Gupta, R. C., "A Study to Establish Correlations between Piezometer Probe Test Results and Insitu Permeability," Master's Thesis, University of Florida, June, 1980.
11. Hirst, T. J., Richards, A. F., and Inderbitzen, A. L., "A Static Cone Penetrometer for Ocean Sediments," ASTM STP 501, American Society for Testing and Materials, 1972, pp. 69-80.
12. Marchetti, S., "A New In Situ Test for the Measurement of Horizontal Soil Deformability," Proceedings Conference on In Situ Measurement of Soil Properties, ASCE Specialty Conference, Raleigh, NC, Vol. 2, June, 1975, PP. 255-259.
13. Marchetti, S., "In Situ Tests by Flat Dilatometer," Journal of the Geotechnical Engineering Division, ASCE, Vol. 106, No. GT3, Proc. Paper 15290, March, 1980, pp. 299-321.
14. "Report of the Subcommittee on Standardization of Penetration Testing in Europe", Proceedings, IXth ICSMFE, Tokyo, Vol. 3, 1977, pp. 95-120.
15. Schmertmann, J. H., "Penetration Pore Pressure Effects on Quasi-Static Cone Bearing, q_c," European Conference on Penetration Testing, Stockholm, Vol. 2, 1974, pp. 345-352.
16. Tumay, M. T., Boggess, R. L., and Acar, Y., "Subsurface Investigations with Piezo-cone Penetrometer," Proceedings ASCE National Convention, St. Louis, MO, 1981, pp. 269-301.
17. Torstensson, B. -A., "Pore Pressure Sounding Equipment," ASCE Speciality Conference on Insitu Measurement of Soil Properties, Raliegh, NC, 1975, pp. 48-55.
18. Wissa, A. E. Z., Martin, R. T., and Garlanger, J. E., "The Piezo-Probe," Proceedings, ASCE Speciality Conference on In Situ Measurement of Soil Properties, Raleigh, NC, Vol. 1, 1975, pp. 536-545.